Int. J. Electrochem. Sci., 7 **(2012)** 8958 - 8973

International Journal of
ELECTROCHEMICAL
SCIENCE
www.electrochemsci.org

Adsorption and Inhibition Effect of 3-Methyl-1-Propargylquinoxalin-2(1H)-One on Carbon Steel Corrosion in Hydrochloric Acid

H. Zarrok[2], *A. Zarrouk*[1,*], *R. Salghi*[3], *Y. Ramli*[4,5], *B. Hammouti*[1], *S. S. Al-Deyab*[6], *E. M. Essassi*[4], *H. Oudda*[2]

[1] LCAE-URAC18, Faculté des Sciences, Université Mohammed 1er, Oujda, Morocco.
[2] Laboratoire des procèdes de séparation, Faculté des Sciences, Université Ibn Tofail, Kénitra, Morocco.
[3] Equipe de Génie de l'Environnement et Biotechnologie, ENSA, Université Ibn Zohr, BP1136 Agadir, Morocco.
[4] Laboratoire de Chimie Organique Hétérocyclique,URAC 21,Université Mohammed V-Agdal ,Rabat ,Morocco et Institute of Nanomatrials and Nanotechnology, MAScIR,Rabat ,Morocco.
[5] Laboratoire Nationale de Contrôle des Médicaments, BP 6206, Rabat, Morocco.
[6] Petrochemical Research Chair, Chemistry Department, College of Science, King Saud University, P.O. Box 2455, Riyadh 11451, Saudi Arabia.
[*]E-mail: azarrouk@gmail.com

Received: 1 August 2012 / *Accepted:* 26 August 2012 / *Published:* 1 September 2012

Inhibition performance of 3-methyl-1-propargylquinoxalin-2(1H)-one (MPQO) against corrosion of carbon steel in 1.0 M HCl was investigated by weight loss and electrochemical measurements. The inhibition efficiency increased with increasing inhibitor's concentration, but decreased with the increase in temperature. The results showed that MPQO acts as a mixed type inhibitor in 1.0 M HCl by suppressing simultaneously the cathodic and anodic processes. Adsorption of used inhibitor led to a reduction in the double layer capacitance and an increase in the charge transfer resistance. Thermodynamic analysis indicates that both physisorption and chemisorption probably occur in the adsorption process. The adsorption behaviour of MPQO follows Langmuir's isotherm.

Keywords: Steel, Hydrochloric acid, Quinoxaline, Polarization curves, EIS.

1. INTRODUCTION

Corrosion inhibitors are of great practical importance, being extensively employed in minimising metallic waste in engineering materials. The wide spread use of carbon steel in a variety of petroleum applications, such as down hole tubular, flow lines and transmission pipelines arewell

known. Hydrochloric acid solutions are widely used in petroleum fields, for cleaning and descaling of iron and steel alloys [1].The use of inhibitors is one of the bestknown methods of corrrosion protection. Organic compounds used as inhibitors act through a process of surface adsorption, so the efficiency of an inhibitor depends not only on the characteristics of the environment in which it acts, the nature of the metal surface and electrochemical potential at the interface, but also on the structure of the inhibitor itself, which includes the number of adsorption active centres in the molecule, their charge density, the molecule size, the mode of adsorption, the formation of metallic complexes and the projected area of the inhibitor on the metal surface [2]. Compounds with functional groups containing hetero-atoms, which can donate lone pair electrons are found to be particularly useful as inhibitors for metal corrosion [3–6]. Recently more study shows that the inhibitive effect is found to enhance several nitrogen containing organic compounds for carbon steel in acid solutions. Organic nitrogen compounds which usually employed for their rapid action in acidic solutions specify the corrosion behaviour of iron and steel [2]. Compounds with π-bonds also generally exhibit good inhibitive properties by providing electrons to interact with metal surface [7–11].

The objective of this investigation is to determine the effect of 3-methyl-1-propargylquinoxalin-2(1H)-one (MPQO) on the corrosion of carbon steel in 1.0 M HCl solution. The corrosion protection effect of MPQO was investigated by means of weight loss measurement, potentiodynamic polarisation, and electrochemical impedance spectroscopy (EIS). The effect of concentration and temperature on the inhibition efficiency has been examined. The thermodynamic parameters for dissolution processes were calculated and discussed. The chemical structure of the studied quinoxaline derivative is given in Fig 1.

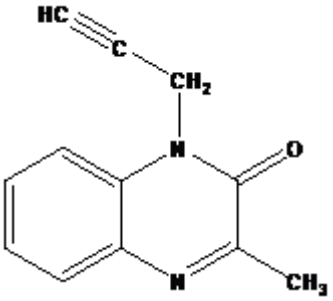

Figure 1. The chemical structure of the studied quinoxaline.

2. EXPERIMENTAL METHODS

2.1. Materials

The steel used in this study is a carbon steel (Euronorm: C35E carbon steel and US specification: SAE 1035) with a chemical composition (in wt%) of 0.370 % C, 0.230 % Si, 0.680 % Mn, 0.016 % S, 0.077 % Cr, 0.011 % Ti, 0.059 % Ni, 0.009 % Co, 0.160 % Cu and the remainder iron (Fe). The carbon steel samples were pre-treated prior to the experiments by grinding with emery paper

SiC (120, 600 and 1200); rinsed with distilled water, degreased in acetone in an ultrasonic bath immersion for 5 min, washed again with bidistilled water and then dried at room temperature before use. The acid solutions (1.0 M HCl) were prepared by dilution of an analytical reagent grade 37 % HCl with double-distilled water. The concentration range of MPQO employed was 10^{-6} M to 10^{-3} M.

2.2. Synthesis

Inhibitors studied are synthesized in our laboratory according to the procedure described in the schemes 1 and 2.

In the literature, 3-methylquinoxalin-2-one is prepared according Philips method [12] scheme1;

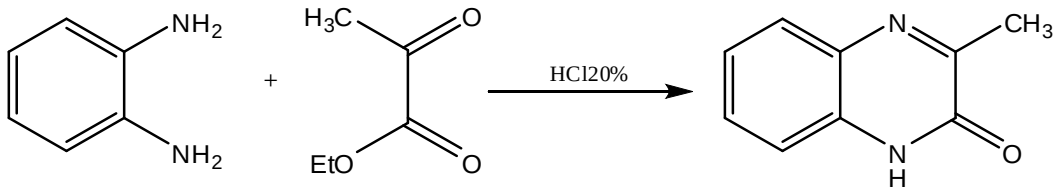

Scheme1. Synthesis of, 3-methylquinoxalin-2-one

To a solution of 3-methylquinoxalin-2(1H)-one (1 g, 6.22 mmol) in DMF (20 ml) was added propargyl bromide (0.82 ml, 6.22 mmol), potassium carbonate (1 g, 7.46 mmol) and a catalytic quantity of tetra-n-butylammonium bromide. The mixture was stirred at room temperature for 24 h. The solution was filtered and the solvent removed under reduced pressure. The residue was recrystallized from ethanol to afford 3-methyl-1-(propargyl)quinoxalin-2(1H)-one as colorless crystals [13] scheme 2.

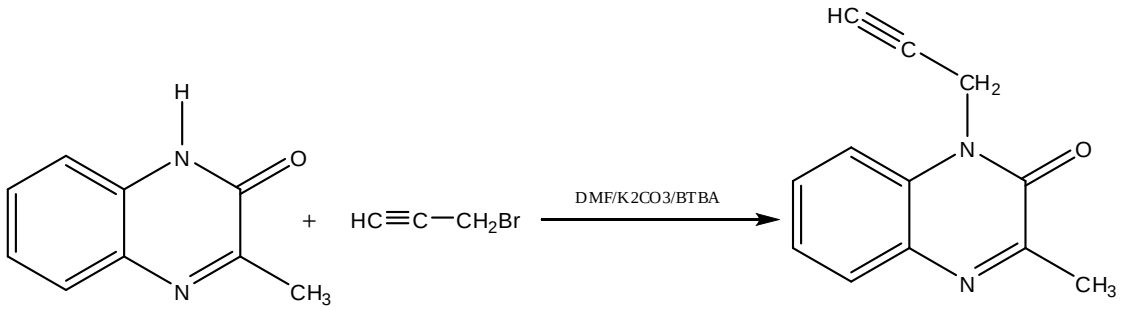

Scheme2. Synthesis of, 3-methyl-1-propargylquinoxalin-2(1H)-one

2.3. Measurements

2.3.1. Weight loss measurements

The gravimetric measurements were carried out at definite time interval of 6 h at room temperature using an analytical balance (precision ± 0.1 mg). The carbon steel specimens used have a

rectangular form (length = 1.6 cm, width = 1.6 cm, thickness = 0.07 cm). Gravimetric experiments were carried out in a double glass cell equipped with a thermostated cooling condenser containing 50 mL of non-de-aerated test solution. After immersion period, the steel specimens were withdrawn, carefully rinsed with bidistilled water, ultrasonic cleaning in acetone, dried at room temperature and then weighted. Triplicate experiments were performed in each case and the mean value of the weight loss was calculated.

2.3.2. Electrochemical measurements

Electrochemical experiments were conducted using impedance equipment (Tacussel-Radiometer PGZ 100) and controlled with Tacussel corrosion analysis software model Voltamaster 4. A conventional three-electrode cylindrical Pyrex glass cell was used. The temperature is thermostatically controlled. The working electrode was carbon steel with the surface area of 1 cm^2. A saturated calomel electrode (SCE) was used as a reference. All potentials were given with reference to this electrode. The counter electrode was a platinum plate of surface area of 1 cm^2. A saturated calomel electrode (SCE) was used as the reference; a platinum electrode was used as the counter-electrode. All potentials are reported *vs*. SCE. All electrochemical tests have been performed in aerated solutions at 308 K.

For polarization curves, the working electrode was immersed in a test solution during 30 min until a steady state open circuit potential (E_{ocp}) was obtained. The polarization curve was recorded by polarization from -600 to -300 mV/SCE with a scan rate of 1 mV s^{-1}). AC impedance measurements were carried-out in the frequency range of 100 kHz to 10 mHz, with 10 points per decade, at the rest potential, after 30 min of acid immersion, by applying 10 mV ac voltage peak-to-peak. Nyquist plots were made from these experiments. The best semicircle can be fit through the data points in the Nyquist plot using a non-linear least square fit so as to give the intersections with the *x*-axis.

3. RESULTS AND DISCUSSION

3.1. Gravimetric study

3.1.1. Effect of quinoxaline derivative on corrosion rate and inhibition efficiency

The gravimetric method (weight loss) is probably the most widely used method of inhibition assessment [14–17]. The simplicity and reliability of the measurement offered by the weight loss method is such that the technique forms the baseline method of measurement in many corrosion monitoring programmes [18].

The corrosion rate (CR) was calculated from the following equation [19, 20]:

$$C_R = \frac{\Delta W}{St} \quad (1)$$

where W is the average weight loss of three carbon steel sheets, S the total area of one carbon steel specimen, and t is the immersion time (6 h). With the calculated corrosion rate, the inhibition efficiency $\eta_{WL}(\%)$ was calculated as follows [21,22]:

$$\eta_{WL}(\%) = \left(1 - \frac{w_i}{w_0}\right) \times 100 \quad (2)$$

where w_0 and w_i are the corrosion rates of the carbon steel coupons in the absence and presence of inhibitor, respectively. Weight loss data of carbon steel in 1.0 M HCl in the absence and presence of various concentrations of inhibitor were obtained and are given in Table 1.

Table 2. Corrosion parameters obtained from weight loss measurements for carbon steel in 1.0 M HCl containing various concentrations of inhibitors at 308 K.

Inhibitor	Conc (M)	*CR* (mg/cm^2 h)	$\eta_{WL}(\%)$	θ
Blank	1	1.070	-----	-----
MPQO	1×10^{-6}	0.443	58.6	0.586
	1×10^{-5}	0.291	72.8	0.728
	5×10^{-5}	0.216	79.8	0.798
	1×10^{-4}	0.200	81.3	0.813
	5×10^{-4}	0.159	85.1	0.851
	1×10^{-3}	0.097	90.9	0.909

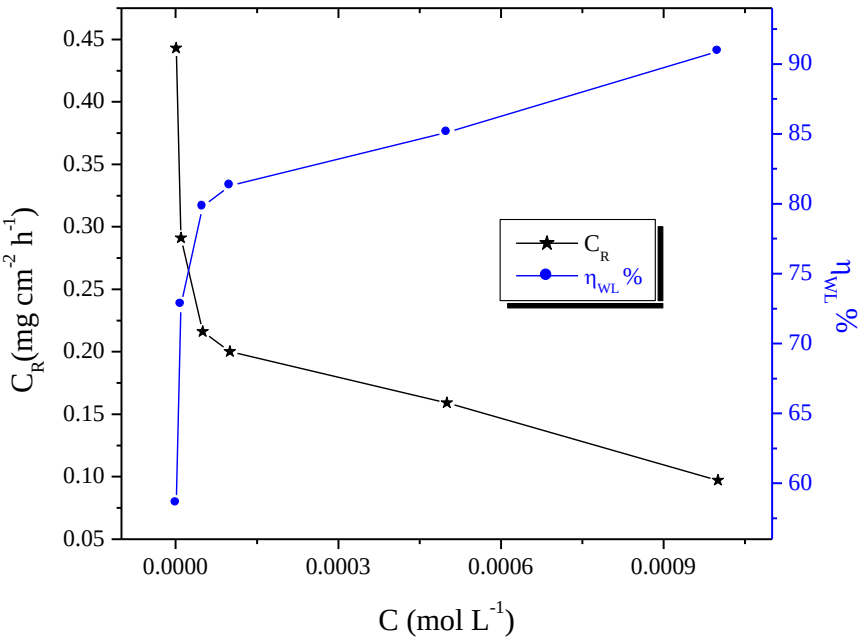

Figure 2. Variation of the corrosion rate and inhibitive efficiency against the MPQO concentrations.

Fig. 2 illustrates the corrosion rate of CRS and inhibition efficiency values obtained from the weight loss in 1.0 M HCl at 308K in the presence of different concentrations of quinoxaline derivative. The corrosion rate reduces after addition of this compound, and decreases with the inhibitor concentration due to the fact that the adsorption coverage increases, which shields the steel surface efficiently from the medium. Indeed, corrosion rate values of carbon steel decrease when the inhibitor concentration increases while $\eta_{WL}(\%)$ values of MPQO increase with the increase of the concentration. The efficiency of an organic compound as corrosion inhibitor depends not only on the characteristics of the environment in which it acts, the nature of the metal surface and electrochemical potential at the interface, but also on the structure of the inhibitor itself, which includes the number of adsorption active centres in the molecule, their charge density, the molecule size, the mode of adsorption, the formation of metallic complexes and the projected area of the inhibitor on the metallic surface [23-29]. The molecular weight of the inhibitor has a direct influence on its inhibition efficiency. The increase in molecular weight of the inhibitor is due to an increase in the length of the hydrocarbon chain of amines [24], nitriles [25] or mercaptants [26]. The rise of the inhibition efficiency is due to the inductive effect of the methyl groups. Quinoxaline compounds are good inhibitors of iron corrosion in hydrochloric acid [30, 31]. Their inhibiting effect is closely related to the molecular structure containing two nitrogen atoms in the quinoxaline ring. The corrosion inhibition can be attributed to the adsorption of the quinoxaline derivative at the steel/acid solution interface.

3.1.2. Effect of temperature

Temperature has a great effect on the corrosion phenomenon. Generally the corrosion rate increases with the rise of the temperature. For this purpose, we made weight loss experiments in the range of temperature 308–343K, in the absence and presence of various concentrations of MPQO after 1 h of immersion.

Table 3. Various corrosion parameters for carbon steel in 1.0 M HCl in the absence and the presence of optimum concentration of MPQO at different temperatures after 1h.

Temp (K)	Inhibitor	C_R (mg/cm^2 h)	η_{WL}%	θ
308	Blank	1.070	-----	-----
	MPQO	0.097	90.9	0.909
313	Blank	1.490	-----	-----
	MPQO	0.237	84.1	0.841
323	Blank	2.870	-----	-----
	MPQO	0.623	78.3	0.783
333	Blank	5.210	-----	-----
	MPQO	1.730	66.8	0.668
343	Blank	10.02	-----	-----
	MPQO	5.962	40.5	0.405

The corresponding data are shown in Table 3. From the Table 3, it is clear that the $\eta_{WL}\%$ decreases with the increase of temperature. The decrease in inhibition efficiency with increase in temperature from 308 to 343K may be probably due to increased rate of desorption of MPQO from the steel surface at [32,33]. The fractional surface coverage θ can be easily determined from weight loss measurements by the ratio $\eta_{WL}\%$ / 100 if one assumes that the values of $\eta_{WL}\%$ do no differ substantially from θ.

In order to calculate activation parameters for the corrosion process, Arrhenius Eq. (3) and transition state Eq. (4) were used [34]:

$$C_R = k \exp\left(-\frac{E_a}{RT}\right) \quad (3)$$

$$C_R = \frac{RT}{Nh} \exp\left(\frac{\Delta S_a}{R}\right) \exp\left(-\frac{\Delta H_a}{RT}\right) \quad (4)$$

where k is the Arrhenius pre-exponential factor, T the absolute temperature, E_a the activation corrosion energy for the corrosion process, h the Planck's constant, N the Avogado's number, ΔS_a the entropy of activation, ΔH_a the enthalpy of activation and C_R is the rate of metal dissolution reaction.

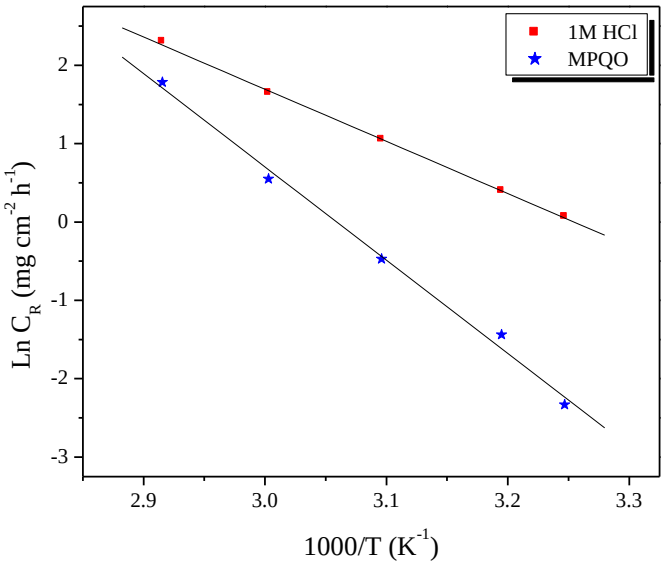

Figure 3. Arrhenius plots of Ln C_R vs. 1/T for steel in 1.0 M HCl in the absence and the presence of MPQO at optimum concentration.

The activation corrosion energy (E_a) of MPQO is calculated by linear regression between Ln(C_R) and 1/T (Fig. 3) and the result is shown in Table 4. The linear regression coefficients are close to 1, indicating that the steel corrosion in hydrochloric acid can be elucidated using the kinetic model. Analysis of the temperature dependence of inhibition efficiency as well as comparison of corrosion

activation energy in absence and presence of inhibitor gave some insight into the possible mechanism of inhibitor adsorption. A decrease in η_{WL}% with rise in temperature, with analogous increase in E_a in presence of inhibitor compared to its absence, is frequently interpreted as being suggestive of formation of an adsorption film of physical (electrostatic) nature. The reverse effect, corresponding to an increase in η_{WL}% with rise in temperature and lower E_a in presence of inhibitor, suggests a chemisorption mechanism [35]. From the foregoing, the trend for 3-methyl-1-propargylquinoxalin-2(1H)-one (MPQO) adsorption onto the carbon steel surface in 1 mol L^{-1} HCl suggests physisorption.

Table 4. Activation parameters for the steel dissolution in 1.0 M HCl in the absence and the presence of MPQO at optimum concentration.

Inhibitors	A (mg/cm^2 h)	Linear regression coefficient (r)	E_a (kJ/mol)	ΔH_a (kJ/mol)	ΔS_a (J/mol K)
Blank	3.0066×10^{9}	0.99961	55.75	53.05	-72.49
MPQO	6.5239×10^{15}	0.99703	98.97	96.27	48.81

Fig. 4 shows a plot of Ln (C_R/T) against 1/T. Straight lines were obtained with a slope is equal to (ΔH_a /R) and intercept is equal to (Ln (R/Nh + ΔS_a /R))), from which the values of ΔH_a and ΔS_a were calculated and listed in Table 4. It is seen that E_a and ΔH_a varied with the same trend and are higher in the presence of inhibitor than in the blank solution, indicating that the energy barrier of the corrosion reaction increased in the presence of MPQO molecule [36]. The positive sign of ΔH_a reflected the endothermic nature of the steel dissolution process suggesting that the dissolution of steel is slow [37] in the presence of inhibitor.

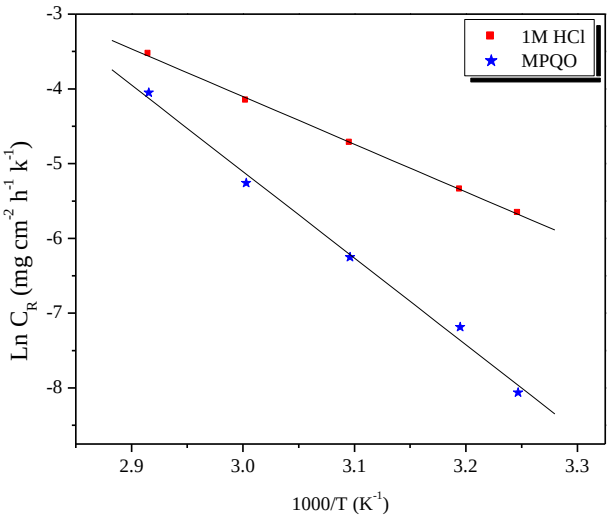

Figure 4. Arrhenius plots of Ln(C_R/T) vs. 1/T for steel in 1.0 M HCl in the absence and the presence of MPQO at optimum concentration.

The value of ΔS_a is lower for the solution without inhibitor than that for the solution with inhibitor. This might be attributed to the rate-determining step for the activated complex was the association rather than the dissociation step [38]. The positive values of ΔS_a reflected the fact that the adsorption process is accompanied by an increase in entropy, which is the driving force for the adsorption of the inhibitor onto the steel surface.

3.1.3. Adsorption isotherm

The action of an inhibitor in aggressive acid media is assumed to be related to its adsorption at the metal/solution interface. The adsorption of an organic adsorbate at a metal/solution interface can be regarded as a substitution adsorption process between the organic molecule in the aqueous solution Org(sol) and the water molecules on the metallic surface $H_2O_{(ads)}$ [39]:

$$Org_{(sol)} + nH_2O_{(ads)} \Leftrightarrow Org_{(ads)} + nH_2O_{(sol)}$$

where $Org_{(sol)}$ and $Org_{(ads)}$ are the organic specie dissolved in the aqueous solution and adsorbed onto the metallic surface, respectively, $H_2O_{(ads)}$ is the water molecule adsorbed on the metallic surface and **n** is the size ratio representing the number of water molecules replaced by one organic adsorbate. To obtain an effective adsorption of an inhibitor on metal surface, the interaction force between metal and inhibitor must be greater than the interaction force of metal and water molecule [40]. The corrosion adsorption processes can be understood using adsorption isotherm. The most frequently used adsorption isotherms are Langmuir, Temkin, and Frumkin. So these adsorption isotherms were tested for the description of adsorption behavior of MPQO on steel surface in HCl solution. The correlation coefficient, R^2, was used to choose the isotherm that best fit experimental data. The fit to the Langmuir isotherm was determined by plotting C_{inh} / θ versus C_{inh} according to the following equation [41]:

$$\frac{C_{inh}}{\theta} = \frac{1}{K_{ads}} + C_{inh} \quad (5)$$

where K_{ads} is the adsorption constant, C_{inh} is the concentration of the inhibitor and surface coverage values (θ) are obtained from the weight loss measurements for various concentrations. The equilibrium constant for adsorption process is related to the free energy of adsorption, ΔG^{o}_{ads}, and is expressed by following equation [42]:

$$LnK_{ads} = Ln\frac{1}{55.5} - \frac{\Delta G^{\circ}_{ads}}{RT} \quad (6)$$

where 55.5 is the molar concentration of water in the solution expressed in M (mol L^{-1}), R is the gas constant (8.314 J K^{-1} mol^{-1}) and T is the absolute temperature (K). The relation between C_{inh}/θ and C_{inh} is shown in Fig. 5. The thermodynamics parameters derived from Langmuir adsorption

isotherm (obtained from weight loss measurements) are given in Table 5. The correlation coefficient, R^2, was used to choose the isotherm that best fits the experimental data. The strong correlation ($R^2 > 0.999$) suggests that the adsorption of inhibitor on the carbon steel surface obeyed this isotherm. The free energy of adsorption value, ΔG°_{ads} was obtained from Eq. (6). Results presented in the Table indicate that the value of ΔG°_{ads} is negative. The negative values also indicate a spontaneous adsorption of the inhibitor molecules.

Table 5. Thermodynamic parameters for the adsorption of MPQO in 1.0 M HCl on the C38 steel at 308K

Inhibitor	Slope	K_{ads} (M^{-1})	R^2	ΔG°_{ads} (kJ/mol)
MPQO	1.10	110372.23	0.99949	-40.02

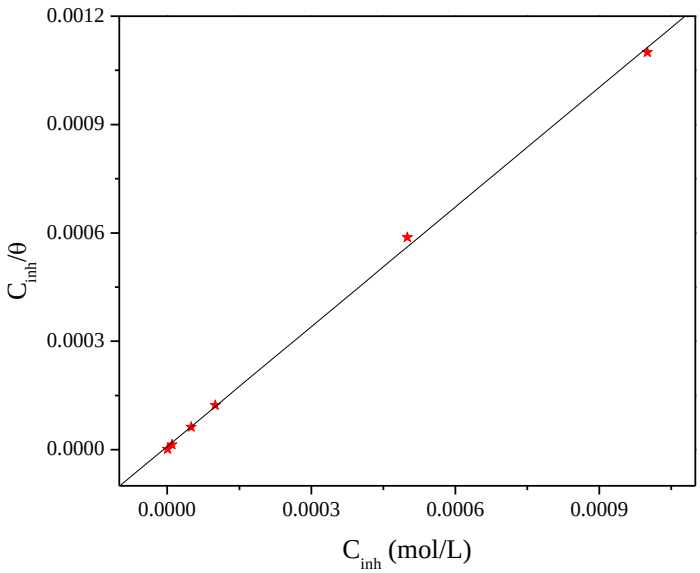

Figure 5. Langmuir adsorption of MPQO on the carbon steel surface in 1.0 HCl solution.

The value K_{ads} calculated from the reciprocal of intercept of isotherm line is indicating in Table 5. The high value of the adsorption equilibrium constant reflects the high adsorption ability of this inhibitor on carbon steel surface. Adsorption of negatively charged species is facilitated if the metal is positively charged. Positively charged species can also protect the positively charged metal surface acting with a negatively charged intermediate such as acid anions adsorbed on the metal surface
[21, 43].

Generally, values of ΔG°_{ads} up to -20 kJ mol^{-1} are consistent with electrostatic interaction between charged molecules and a charged metal (which indicates physical adsorption) while those

more negative than -40 kJ mol^{-1} involves charge sharing or transfer from the inhibitor molecules to the metal surface to form a co-ordinate type of bond (which indicates chemisorption) [21]. The calculated standard free energy of adsorption value is closer to -40 kJ mol^{-1}. This value is in frontier between the two modes of adsorption, therefore, it can be concluded that the adsorption is a competitive phenomenon between chemical and physical adsorption [44, 45]. We may also introduce the interamolecular synergistic effect between propargylic and quinoxaline well known in literature as corrosion inhibitors [30,31, 46].

3.2. Tafel polarization study

Potentiodynamic polarization curves of carbon steel in 1.0 M HCl containing MPQO at 308K are shown in Fig. 6, respectively. In all cases, addition of this compound causes a remarkable decrease in the corrosion rate i.e., shifts the both anodic and cathodic curves to lower current densities. In other words, both cathodic and anodic reactions of carbon steel electrode are drastically inhibited by the quinoxaline compound. It should be noted that in anodic domain, it is difficult to recognize the linear Tafel regions. Accordingly, the corrosion current density values are estimated accurately by extrapolating the cathodic linear region back to the corrosion potential. Similar fitting method has also been widely used [47]. The electrochemical corrosion parameters including corrosion current density (I_{corr}), corrosion potential (E_{corr}), cathodic Tafel slope (β_c) and inhibition efficiency ($\eta_{Tafel}(\%)$) values were derived from cathodic current–potential curves are presented in Table 6. The $\eta_{Tafel}(\%)$ was calculated from polarization measurements according to the relation given below;

$$\eta_{Tafel}(\%) = \frac{I_{corr} - I_{corr(i)}}{I_{corr}} \times 100 \quad (7)$$

where I_{corr} and $I_{corr(i)}$ are the corrosion current densities for steel electrode in the uninhibited and inhibited solutions, respectively.

The analyses of the data in Table 6, revealed that the I_{corr} decreases considerably with increasing MPQO concentration. In Table 6, I_{corr} value decreases from 1077.8 to 89.5 μA cm^{-2} with the highest concentration of MPQO (10^{-3}M). The obtained efficiencies ($\eta_{Tafel}(\%)$) indicate that MPQO acts as an effective inhibitor. The values of $\eta_{Tafel}(\%)$ increase with the inhibitor concentration reaching its maximum value, 91.7% at 10^{-3}M. An increase in the inhibitor concentration probably increased the number of inhibitor molecules on the surface and thus decreased the corrosion current density. It can be concluded that this inhibitor acts through adsorption on carbon steel surface and formation of a barrier layer on the metal surface. The presence of MPQO does not prominently shift the corrosion potential, which indicates the studied quinoxaline derivative act as mixed-type inhibitor [48]. Furthermore, in the presence of this inhibitor, the slight change of β_c indicates that the cathodic corrosion mechanism of steel does not change.

Table 6. Polarization data of C38 steel in 1.0 M HCl without and with addition of inhibitor at 308 K.

Inhibitor	Conc (M)	$-E_{corr}$ (mV/SCE)	$-\beta_c$ (mV dec^{-1})	I_{corr} ($\mu A\ cm^{-2}$)	η_{Tafel} (%)
HCl	1	475.9	176	1077.8	-
MPQO	10^{-3}	471.1	168	089.5	91.7
	10^{-4}	474.0	188	208.5	80.6
	10^{-5}	492.3	156	315.3	70.7
	10^{-6}	493.2	190	458.5	57.5

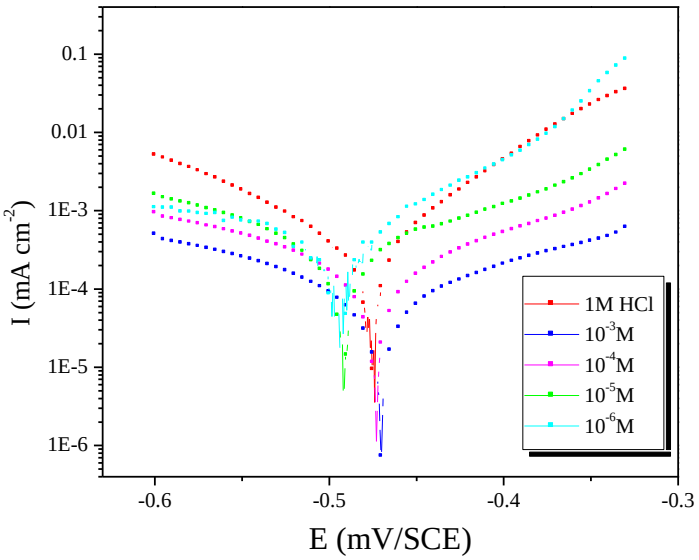

Figure 6. Polarisation curves of carbon steel in 1.0 M HCl for various concentrations of MPQO.

3.3. Electrochemical impedance spectroscopy (EIS) studies

EIS has also been used for the investigation of inhibition performance of MPQO. Nyquist plots for carbon steel in 1.0 M HCl solutions with and without inhibitor are shown in Fig. 7. These diagrams merely present a capacitive loop in the first quadrant, indicating that there is only one time constant. As shown in Fig. 7, the capacitive loops are slightly depressed as semi-circular shapes because of the roughness and other inhomogeneities of carbon steel surface resulting in a phenomenon called ‘‘dispersing effect’’ [49,50]. It is apparent that the impedance response of carbon steel has significantly changed after the addition of MPQO. The diameters of those loops increase with increasing concentrations of MPQO. The impedance data are analyzed based on the electrochemical equivalent circuit shown in Fig. 8. R_s represents the electrolyte resistance, R_p is the polarization resistance, CPE represents constant phase element to replace a double layer capacitance (C_{dl}) for more accurate fit. The impedance of a constant phase element is described by the expression:

$$Z_{CPE} = Y_0^{-1}(j\omega)^{-n} \quad (8)$$

where Y_0 is a proportional factor, n has the meaning of a phase shift. For n = 0, CPE represents a resistance, for n = 1 a capacitance, for n = 0.5 a Warburg element and for n = -1 an inductance. The impedance parameters derived from these plots are given in Table 7. The double layer capacitance (C_{dl}) and inhibition efficiency (η(%)) are defined as follows:

$$C_{dl} = Y_0 (\omega_m^{''})^{n-1} \quad (9)$$

$$\eta\% = (\frac{R_p^{'} - R_p}{R_p^{'}}) \times 100 \quad (10)$$

where $\omega_m^{''}$ is the angular frequency at which the imaginary part of the impedance has a maximum. $R_p^{'}$ and R_p are the values of polarization resistance in the absence and presence of inhibitor, respectively.

In EIS, value of R_p reflects the degree of difficulty in corrosion reaction, the higher the value is, the lower the corrosion rate is. It can be seen from Table 7 that the value of R_p increases significantly with increasing concentrations of MPQO, which demonstrates that the inhibitor prevents the corrosion reaction effectively. Additionally, the value of C_{dl} decreases with increasing concentrations of inhibitor, which can be attributed to the decrease in local dielectric constant or an increase in the thickness of the electrical double layer. This result, therefore, suggests that MPQO molecules function by adsorption at the interface of metal/solution as a consequence of replacement of water molecules by MPQO molecules [51].

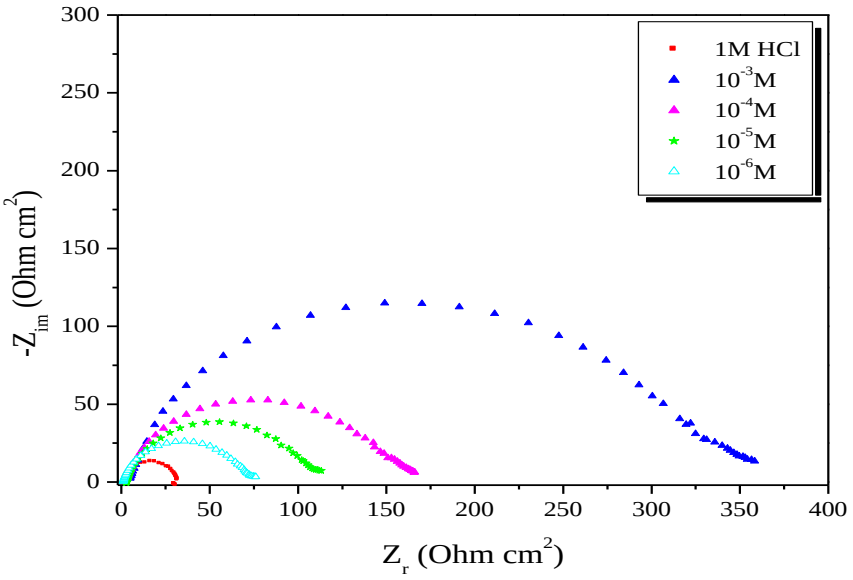

Figure 7. Nyquist diagrams for carbon steel in 1.0 M HCl containing different concentrations of MPQO at 308 K.

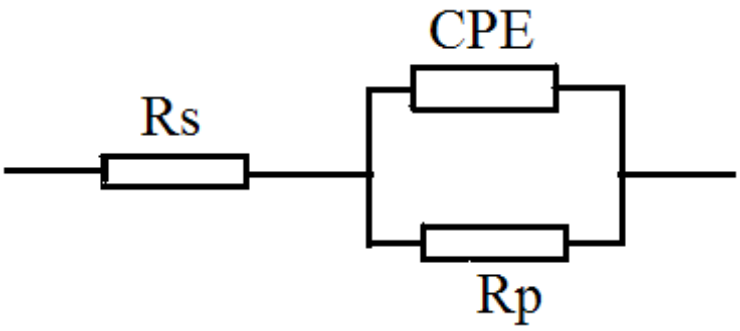

Figure 8. Equivalent circuit model used to fit the impedance spectra.

Table 7. Electrochemical impedance parameters for carbon steel in 1.0 M HCl in absence and presence different concentrations of inhibitor.

Inhibitor	Conc (M)	R_s (Ω cm^2)	R_p (Ω cm^2)	f_{max} (Hz)	C_{dl} (μF cm^{-2})	η (%)
HCl	1	1.6	031.0	63.3	80.99	-
MPQO	10^{-3}	0.5	351.8	25.0	18.10	91.2
	10^{-4}	0.4	163.5	31.6	30.80	81.0
	10^{-5}	1.2	109.7	31.6	45.90	71.7
	10^{-6}	1.0	074.0	40.0	53.80	58.1

The results obtained from the EIS technique in 1.0 M HCl solution were in good agreement with those obtained from weight loss method and potentiodynamic polarization method.

4. CONCLUSION

MPQO was proved to be an effective inhibitor for the corrosion of carbon steel at different temperatures in 1.0 M HCl solution. Inhibition efficiency increases with increasing inhibitor concentration but decreases with rise in temperature. MPQO acts as a mixed-type corrosion inhibitor, inhibiting the anodic and cathodic processes of the corrosion reactions by forming a protective film on metal surface. The adsorption model obeyed Langmuir adsorption isotherm. The negative values of ΔG°_{ads} indicated a spontaneous adsorption of the inhibitor on the surface of steel. The inhibition efficiencies obtained from EIS, Tafel polarisation and weight loss methods are in reasonable agreement with each other.

ACKNOWLEDGEMENTS
Prof S. S. Al-Deyab and Prof B. Hammouti extend their appreciation to the Deanship of Scientific Research at king Saud University for funding the work through the research group project.

References

1. M.A. Migahed, *Mater. Chem. Phys*. 93 (2005) 48.
2. A.Chetouani, B. Hammouti, T. Benhadda, M. Daoudi, *Appl. Surf. Sci*. 249 (2005) 375.

3. H. Zarrok, S. S. Al-Deyab, A. Zarrouk, R. Salghi, B. Hammouti, H. Oudda, M. Bouachrine, F. Bentiss, *Int. J. Electrochem. Sci*. 7 (2012) 4047.
4. H. Zarrok, H. Oudda, A. El Midaoui, A. Zarrouk, B. Hammouti, M. Ebn Touhami, A. Attayibat, S. Radi, R. Touzani, *Res. Chem. Intermed*. (2012) DOI: 10.1007/s11164-012-0525-x).
5. H. Zarrok, R. Salghi, A. Zarrouk, B. Hammouti, H. Oudda, Lh. Bazzi, L. Bammou, S. S. Al-Deyab. *Der Pharm. Chem*. 4 (2012) 407.
6. A.Ghazoui, R. Saddik, N. Benchat, B. Hammouti, M. Guenbour, A. Zarrouk, M. Ramdani, *Der Pharm. Chem.* 4 (2012) 352.
7. Zarrouk, B. Hammouti, H. Zarrok, R. Salghi, A. Dafali, Lh. Bazzi, L. Bammou, S. S. Al-Deyab, *Der Pharm. Chem*. 4 (2012) 337
8. H. Zarrok, S. S. Al-Deyab, A. Zarrouk, R. Salghi, B. Hammouti, H. Oudda, M. Bouachrine, F. Bentiss, *Int. J. Electrochem. Sci*. 7 (2012) 4047.
9. H. Zarrok, H. Oudda, A. El Midaoui, A. Zarrouk, B. Hammouti, M. Ebn Touhami, A. Attayibat, S. Radi, R. Touzani, *Res. Chem. Intermed*. (2012) DOI: 10.1007/s11164-012-0525-x).
10. H. Zarrok, R. Salghi, A. Zarrouk, B. Hammouti, H. Oudda, Lh. Bazzi, L. Bammou, S. S. Al-Deyab. *Der Pharm. Chem*. 4 (2012) 407.
11. A.Zarrouk, B. Hammouti, H. Zarrok, R. Salghi, A. Dafali, Lh. Bazzi, L. Bammou, S. S. Al-Deyab, *Der Pharm. Chem*. 4 (2012) 337.
12. MA. Philips, *J. Chem. Soc.* 203 (1928) 2393.
13. . Hanane Benzeid, Youssef Ramli, Laure Vendier, El Mokhtar Essassi and Seik Weng Ng, *Acta. Cryst*. 65 (2009) o2196.
14. A.Y. Musa, A.A. Khadom, A.H. Kadhum, A.B. Mohamad, M.S. Takriff, *J. Taiwan, Ins. Chem. Eng*. 41 (2010) 126.
15. A. A. Khadom, A.S. Yaro, A.H. Kadum, J. Taiwan, *Ins. Chem. Eng*. 41 (2010) 122.
16. M. Bouklah, B. Hammouti, M. Lagrenee, F. Bentiss, *Corros. Sci*. 48 (2006) 2831.
17. S. Chitra, K. Parameswari, C. Sivakami, A. Selvaraj, *Chem. Eng. Res. Bull*. 14 (2010) 1.
18. A.R. Afidah, J. Kassim, *Recent Patents Mater. Sci*. 1 (2008) 223.
19. S.A. Umoren, M.M. Solomon, I.I. Udousoro, A.P. Udoh, *Cellulose.* 17 (2010) 635.
20. M.M. Solomon, S.A. Umoren, I.I. Udosoro, A.P. Udoh, *Corros. Sci*. 52 (2010) 1317.
21. S.A. Umoren, I.B. Obot, E.E. Ebenso, N.O. Obi-Egbedi, *Desalination.* 247 (2009) 561.
22. S.A. Umoren, I.B. Obot, N.O. Obi-Egbedi, *J. Mater. Sci*. 44 (2009) 274.
23. A. Gadallah, M.W. Badawy, H.H. Reban, M.M. Abouromia, *J. Appl. Electrochem.* 19 (1989) 928.
24. S. Sankarapapavinasan, F. Pishapinadon, M.F. Ahmed, *Corrosion. Sci*. 32 (1991) 193.
25. V. Carassiti, F. Zucchi, G. Trabanelli, 3 SEIC, Ann. Univ. Ferrara, N.S. Sez.V, Suppl. N. 5, 1970, p. 525.
26. G. Trabanelli, F. Zucchi, G. Gullini, V. Carassiti, *Werkst und Korrosion*. 20 (1968) 407.
27. E. Stupnisek Lisac, M. Metikos-Hakovic, D. Lencic, J. Vorkapic-Farac, K. Berkovic, *Corrosion*. 48 (1992) 924.
28. A. Aouniti, B. Hammouti, M. Brighli, S. Kertit, F. Berhili, S. El Kadiri, A. Ramdani, *J. Chim. Phys*. 93 (1996) 1262.
29. B. Hammouti, R. Salghi, S. Kertit, *J. Electrochem. Soc. of India*. 47 (1998) 31.
30. M. Benabdellah, R. Touzani, A. Aouniti, A. Dafali, S. Elkadiri, B. Hammouti, M. Benkaddour, *Phys. Chem. News*. 37 (2007) 63.
31. M. Benabdellah, K. Tebbji, B. Hammouti, R. Touzani, A. Aouniti, A. Dafali, S. El Kadiri, *Phys. Chem. News.* 43 (2008) 115.
32. X. Li, S. Deng, H. Fu, *Prog. Org. Coat*. 67 (2010) 420.
33. I.B. Obot, N.O. Obi-Egbedi, *Curr. Appl. Phys*. 11 (2011) 382.
34. M. Behpour, S.M. Ghoreishi, M. Khayat Kashani, N. Soltani, *Mater. Corros*. 60 (2009) 895.
35. E.E. Ebenso, *Corros. J*. 1 (1998) 29.
36. S.T. Arab, K.M. Emran, *Inter. J. App. Chem*. 3 (2007) 69.

37. N.M. Guan, L. Xueming, L. Fei, *Mater. Chem. Phys*. 86 (2004) 59.
38. X. Li, S. Deng, H. Fu, G. Mu, *Corros. Sci*. 50 (2008) 2635.
39. M. Behpour, S.M. Ghoreishi, A. Gandomi-Niasar, N. Soltani, M. Salavati-Niasari, *J. Mater. Sci*. 44 (2009) 2444.
40. V.S. Sastri, E. Ghali, M. Elboujdaini, Corrosion Prevention and Protection Practical Solutions, John Wiley & Sons Ltd., 2007. p. 84.
41. E. Bayol, K. Kayakırılmaz, M. Erbil, *Mater. Chem. Phys*. 104 (2007) 74.
42. S.A. Ali, M.T. Saeed, S.U. Rahman, *Corros. Sci*. 45 (2003) 253.
43. M. Behpour, S.M. Ghoreishi, M. Khayatkashani, N. Soltani, *Corros. Sci*. 53 (2011) 2489.
44. A. Yurt, A. Balaban, S. Ustun Kandemir, G. Bereket, B. Erk, Mater. Chem. Phys. 85 (2004) 420.
45. X. Li, S. Deng, H. Fu, T. Li, *Electrochim. Acta*. 54 (2009) 4089.
46. Y. Feng, K.S. Siow, W.K. Teo, A.K. Hsieh, *Corros. Sci*. 41 (1999) 829.
47. P.C. Okafor, Y.G. Zheng, *Corros. Sci*. 51 (2009) 850.
48. C. Cao, *Corros. Sci*. 38 (1996) 2073.
49. S. Ramesh, S. Rajeswari, *Electrochim. Acta*. 49 (2004) 811.
50. M.E. Achouri, S. Ketit, *Prog. Org. Coat*. 43 (2001) 267.
51. X. Wang, H. Yang, F. Wang, *Corros. Sci*. 53 (2011) 113.